ANALYSIS OF COMPLEX AERODYNAMIC CONFIGURATIONS WITH A ZONAL NAVIER-STOKES SOLVER

Turgut Serkan ŞEN[1], Bülent KORKEM[2]
TAI-TUSAŞ Aerospace Industries Inc., P.O. Box 18, 06692, Ankara, TÜRKİYE

Beytullah TEMEL[3]
TÜBİTAK-SAGE, P.K. 16, 06261, Ankara, TÜRKİYE

M. Şerif KAVSAOĞLU[4]
Middle East Technical University, Dept. of Aeronautical Engineering
06531, Ankara, TÜRKİYE

Abstract

The flow fields around different aerodynamic bodies have been solved. The steady state solutions were obtained by using two and three dimensional, multi-zone, time marching, Reynolds averaged Thin Layer Navier-Stokes codes with Beam-Warming finite difference implicit algorithm and Baldwin-Lomax, Cebeci-Smith and Johnson-King turbulence models. The matrix solution is carried out using a diagonally dominant LU-ADI factorization algorithm. The computations around various geometries were performed at well known test cases. The results were compared with experimental and other numerical results.

Introduction

In the last decade, Computational Fluid Dynamics (CFD) has become a part of the aerodynamic design process as a result of the improvements in numerical algorithms, grid generation, computer processing power and post processing graphics. Even though CFD is used for wide variety of applications, there are still many obstacles to overcome. Since the concept of body fitted coordinate transformation has been introduced, structured grid methods became the most popular CFD methods. But increasing demand for more realistic and complex applications forced researchers to seek out alternatives to overcome the inadequacy of these methods. As the flow field becomes more and more complicated, even the sophisticated grid generation codes can not supply reasonable meshes for the simulation. On the other hand, computer speed and memory limitations may restrict the dynamic data storage. Multi block grid generation and implementation to the flow solvers is a good alternative which can overcome the difficulties encountered in a single block solution.

In the present study, a single block thin layer Navier-Stokes code has been modified to a zonal solver. In the grid generation, whole domain is divided into non overlapping, geometrically simpler sub-regions or zones.

Solution Method

The governing equations are written in curvilinear coordinates with strong conservation form for shock capturing purposes,

$$Q_\tau + E_\xi + F_\eta + G_\zeta = \frac{k}{\mathrm{Re}}\left(S_{1_\xi} + S_{2_\eta} + S_{3_\zeta}\right) \qquad (1)$$

where $k = \begin{cases} 0 & \text{for inviscid} \\ 1 & \text{for viscous} \end{cases}$

Here Q is the dependent variable vector, J is the transformation Jacobian,

$$Q = J^{-1}[\rho, \rho u, \rho v, \rho w, e]^T \qquad (2)$$

and E, F, G are the inviscid flux vectors, S_1, S_2, S_3 are the thin layer viscous flux vectors in each curvilinear direction, and Re is the Reynolds number.

The matrix solution is carried out using a diagonally dominant Lower-Upper bi-diagonal ADI (LU-ADI) [1] factorization algorithm. This algorithm requires less memory storage as well as less computing time which has made the practical computations possible. The present LU-ADI factorization simplifies inversion works for the left hand side operators of the most commonly used Beam-Warming [2] scheme. Each ADI operator is decomposed to the product of lower and upper bi-diagonal matrices. The explicit part of the delta form equation is the same as that of Beam-Warming scheme where central difference is used. The method is first order accurate in time and second order accurate in space. Convergence, stability and smoothness of the solution may depend on the implicit and explicit smoothing factors and CFL number;

---

[1]Design Engineer, also Ph.D. student at M.E.T.U. Aeronautical Eng. Dept., Ankara, Türkiye

[2]Sr. Design Engineer, also M.S. student at M.E.T.U. Aeronautical Eng. Dept., Ankara, Türkiye

[3]Research Engineer, also M.S. student at M.E.T.U. Aeronautical Eng. Dept., Ankara, Türkiye

[4]Associate Professor, also consultant at TÜBITAK-SAGE, Ankara, Türkiye, Member AIAA

$$CFL = \frac{\Delta t \cdot \sigma_{max}}{\min\left(\Delta_\xi, \Delta_\eta, \Delta_\zeta\right)} \quad (3)$$

where σ_{max} is the maximum eigen value.

Multiblock Technique

The idea of multiple zone technique is to reduce a geometrically complex region into several smaller and more manageable regions. Grids can be independently generated for each zone. In the present zonal scheme, the flow field is divided into conceivable structures provided that cell to cell matching on block boundaries is maintained. The requirement of cell matching is chosen to eliminate complex interpolation processes at the matched faces of two adjacent zones [3]. The grid points were clustered near the surface and near intersected faces of neighbor zones. Also in a direction normal to surface, the grid points have to be clustered at the surface in order to resolve turbulent boundary layer.

Results

The selected configurations are; NACA0012 airfoil, single flapped airfoil (NLR 7301), ONERA-M6 wing, sharp-edged delta-rectangular wing, a wing-body configuration, and a wrap-around finned missile. The computations for these geometries were performed in a wide range of angles of attack and free stream Mach numbers. The solutions were compared with available experimental and numerical results. The numerical computations were found to agree well with these results.

NACA0012 Airfoil

The NACA0012 airfoil computations were performed at three different flight conditions:

A. M=0.550, α=8.34 deg.
B. M=0.700, α=1.49 deg.
C. M=0.799, α=2.26 deg.

For all cases the Reynolds number is 9×10^6. A single zone hyperbolic C-type grid was used with the dimensions of 161×61. Three different turbulence models were used (Baldwin-Lomax [4] , Cebeci-Smith [6] and Johnson-King [7]) to simulate the turbulence effects. The BL and CS turbulence models are equlibrium models and the JK model is half-equation non-equilibrium model. The aerodynamic coefficients of computations were compared to the experiment [8] in Table 1. In the first two solutions, the three turbulence models agree well with the experiment. But in the third case, the equilibrium turbulence models (BL and CS) predict a shock wave that are too far downstream and very weak separation. On the other hand, the non-equilibrium model (JK) predicts the shock wave location and the shock induced separation well. A sample grid and computed pressure coefficients with BL, CS and JK turbulence models compared to experimental data, were presented in Figure 1a-b.

Mach	α°	Computation		Experiment	
		C_L	C_D	C_L	C_D
0.550	8.34	0.9727	0.0419	0.9750	0.0350
0.700	1.49	0.2450	0.0091	0.2410	0.0079
0.799	2.26	0.3715	0.0317	0.3900	0.0331

TABLE 1 - Comparison of Aerodynamic Coefficients

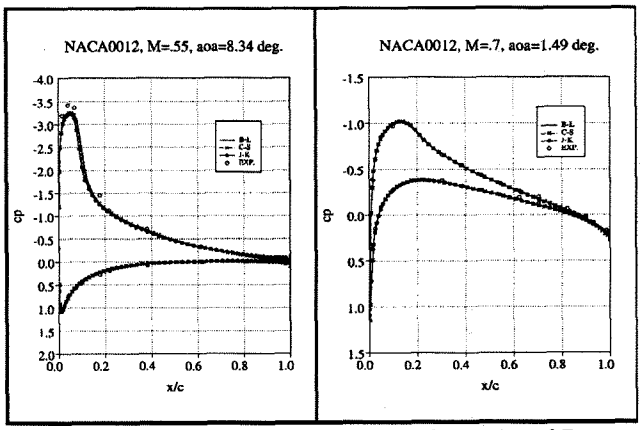

FIGURE 1a - C_p Distributions for Cases A and B

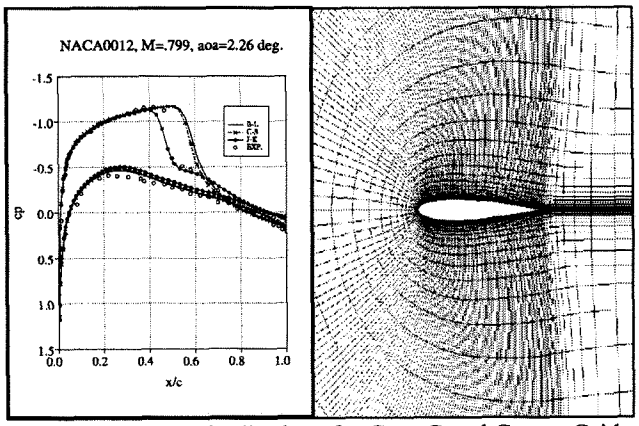

FIGURE 1b - C_p Distributions for Case C and C-type Grid

NLR 7301 Single Flapped Airfoil

This case is a low speed multi-element airfoil computation test case.The basic airfoil section is the NLR7301 with trailing edge flap. The flap chord is 32% of the main airfoil and is deflected 20 degrees down. The flap gap is 2.6% of the main airfoil chord and the Reynolds number based on chord length is 2.51×10^6. The computation was performed at M=0.185, α=6 degrees with the BL turbulence model only. The computational grid system shown in Figure 2 , is composed of 5 blocks with the dimensions given in Table 2 (streamwise and normal directions respectively). The Mach contours, velocity vectors at leading and trailing edges, streamline patterns, and surface pressure coefficient distribution were shown through Figure 3 to Figure 5. The experimental data is taken from Reference [9]. The difference between computation and experiment is due to lack of far field corrections at the outer boundary.

Block #	ξ direction	η direction
1	101	49
2	115	25
3	65	25
4	51	49
5	51	25

TABLE 2 - Grid Dimensions in Each Zone

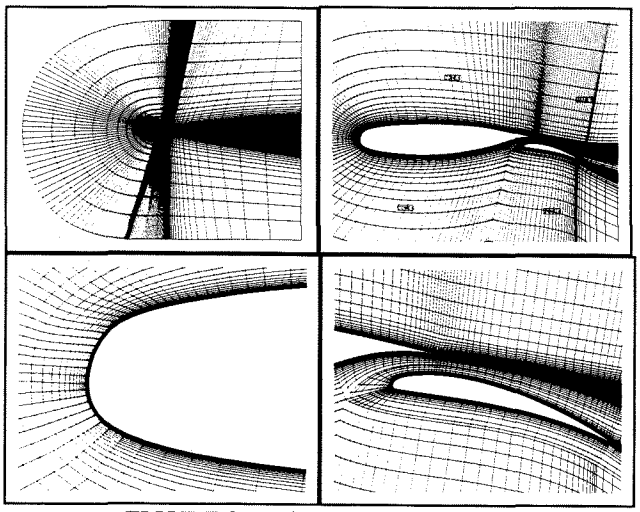

FIGURE 2 - Grid Around NLR 7301

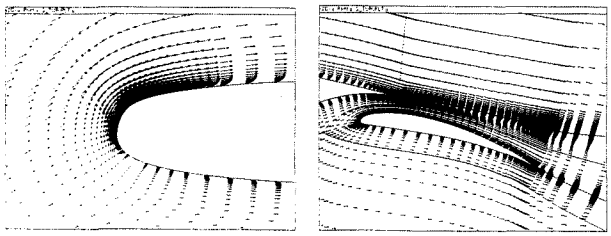

FIGURE 3 -Velocity Vectors over NLR 7301

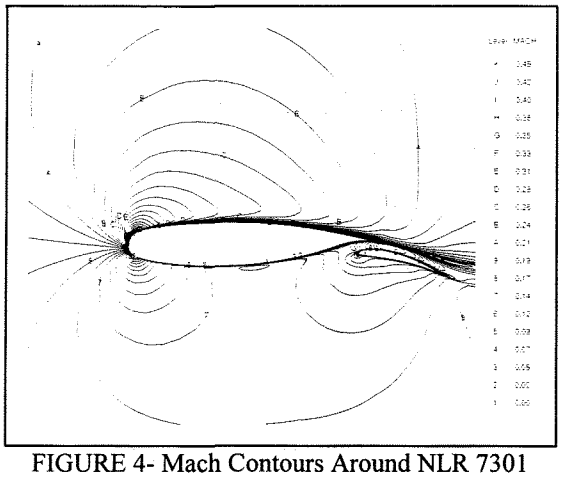

FIGURE 4- Mach Contours Around NLR 7301

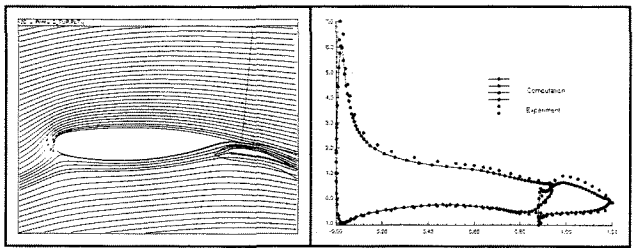

FIGURE 5- -Streamline Pattern and C_p Distribution over NLR 7301

Sharp-Edged Wing

The sharp-edged wing geometry was chosen from a NASA wind tunnel test case to verify present zonal code. The details of this geometry is given in Figure 6. The body fitted computational multi zone grid is shown in Figure 7. The calculations were performed at a fixed Mach number of 2.16 and Reynolds number of 1.33×10^6, and angles of attack α = 1.3, 6.3, 11.3 degrees with a total mesh size of 262564 points (see Table 3). A comparison of computed and experimental spanwise surface pressure distributions at $M_\infty = 2.16$ and $\alpha = 6.3°$ was presented in Figure 8. Pressure coefficient contours were given in Figure 9. Also the lift coefficients are compared with the available experimental [10], and numerical [11] results in Table 4.

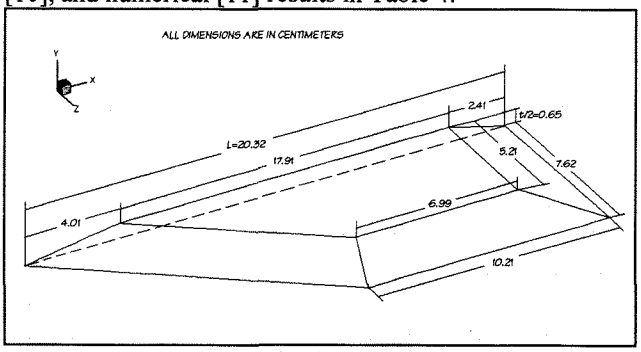

FIGURE 6 -Sharp-Edged Delta-Rectangular Wing

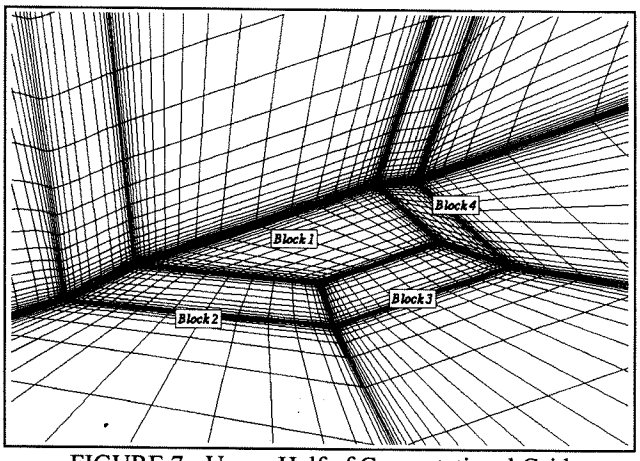

FIGURE 7 - Upper Half of Computational Grid

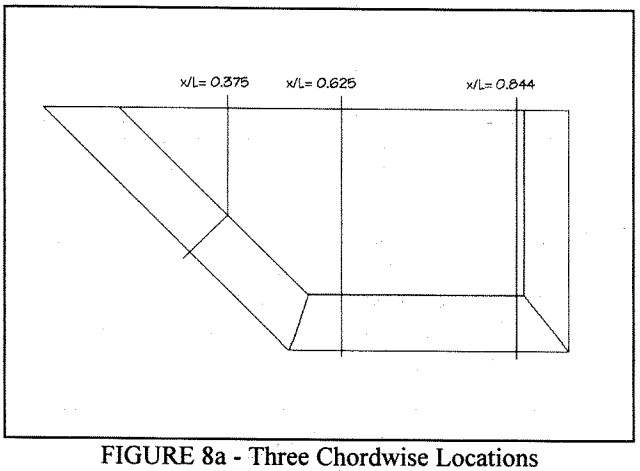

FIGURE 8a - Three Chordwise Locations

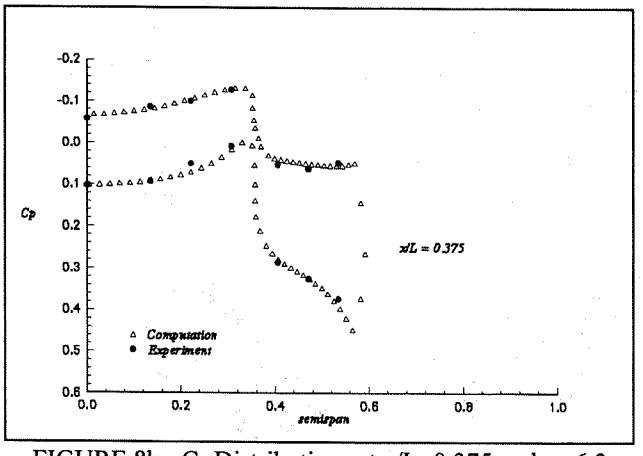

FIGURE 8b - C_p Distributions at x/L=0.375 and α=6.3

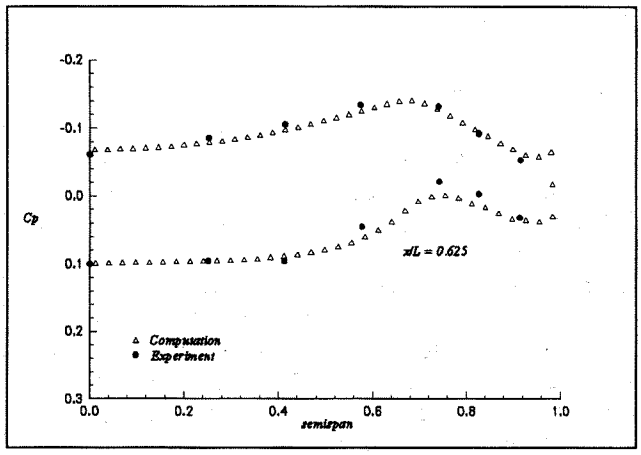

FIGURE 8c - C_p Distributions at x/L=0.625 and α=6.3

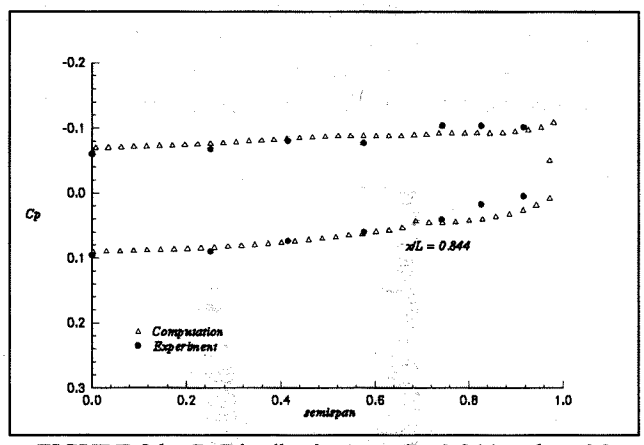

FIGURE 8d - C_p Distributions at x/L=0.844 and α=6.3

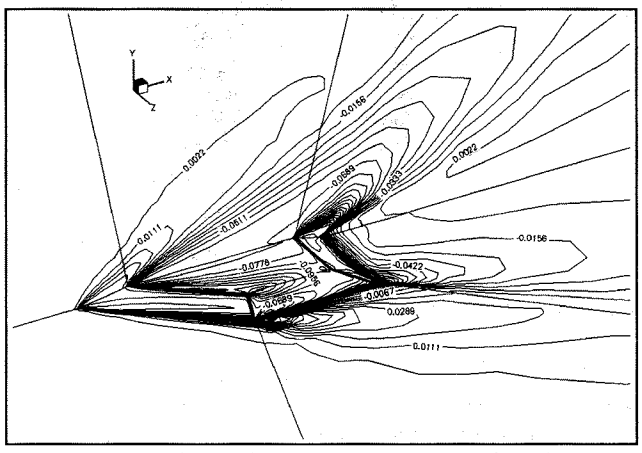

FIGURE 9 - C_p Contours at M=2.16 and α=6.3

Block #	ξ direction	η direction	ζ direction
1 and 5	25	23	41
2, 4, 6 and 8	37	23	41
3 and 7	37	25	41

TABLE 3 - Grid Dimensions in Each Zone

α	Present C_L	Experimental C_L[8]	Computed C_L[9]
1.3	0.033	0.030	0.034
6.3	0.168	0.164	0.168
11.3	0.305	0.308	0.306

TABLE 4 - C_L Comparison for Sharp-Edged Wing

ONERA-M6 Wing

The ONERA-M6 wing computations were performed at three different test case conditions :

A. M=0.84, α=3.06 deg.
B. M=0.84, α=5.06 deg.
C. M=0.84, α=6.06 deg.

For all cases the Reynolds number is 11.7×10^6. The first case is known as the attached flow case and was computed with BL and JK turbulence models, the C_p distributions along span were presented for both models, but the particle traces and the surface pressure distributions were only presented for the BL turbulence model. The other two cases are separated flow cases and were computed using only the BL turbulence model. The computational grid system shown in Figure 10 is a single block mesh which is hyperbolic C-type in streamwise and normal directions and algebraic O-type in spanwise direction, and dimensioned as 181×51×41 in streamwise, spanwise and normal directions respectively.The distance to the outer boundary is 6 root chords and the first point off the body is 4×10^{-3}. The experimental data are taken from references [12] and [13].

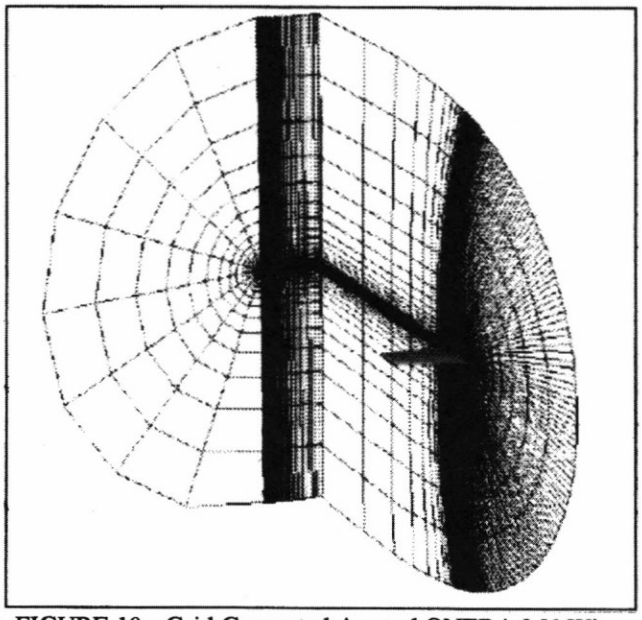

FIGURE 10 - Grid Generated Around ONERA-M6 Wing

The pressure coefficient comparisons for the attached flow case were done at 20%, 44%, 65% and 80% spanwise positions. These pressure coefficient comparisons were presented in Figure 11. The computational results obtained with BL and JK turbulence models for the attached flow case show good agreement with experimental data.

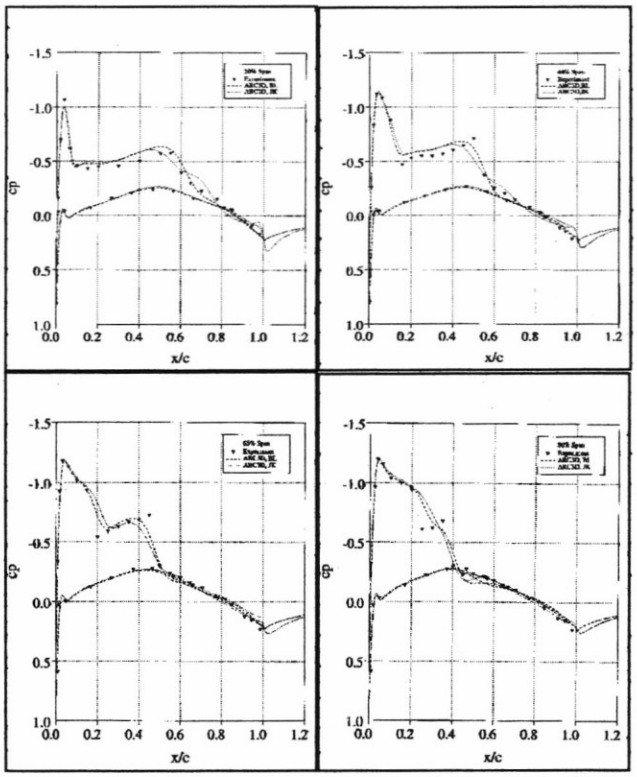

FIGURE 11 - C_P Distributions at Different Spanwise Locations on ONERA-M6 Wing for Case A

In Figures 12 and 13, the experimental and computational particle traces and the surface pressure distributions were presented. The particle traces show that there separation for this case. The surface pressure distribution locate the shock wave on the wing.

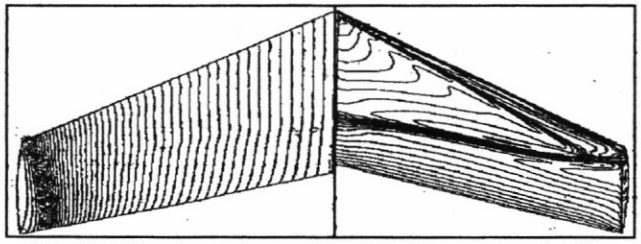

FIGURE 12 - Experimental Particle Traces and Surface Pressure Distribution on ONERA-M6 Wing for Case A

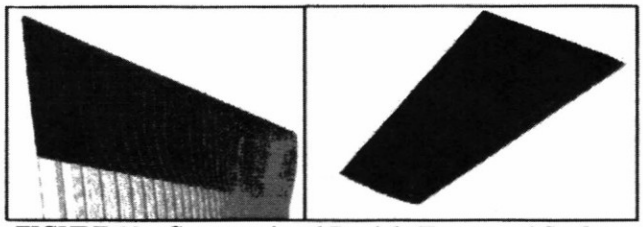

FIGURE 13 - Computational Particle Traces and Surface Pressure Distribution on ONERA-M6 Wing for Case A

The mild separation case was presented as only particle traces, Figure 14, and this figure also has the tendency as is on the experimental data that there exists shock induced separation towards the wing tip.

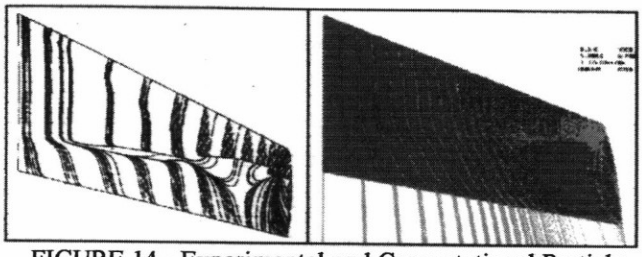

FIGURE 14 - Experimental and Computational Particle Traces on ONERA-M6 Wing for Case B

The separated flow case was also computed with BL turbulence model only and the Figure 15 shows the lambda shock over the wing and Figure 16 demonstrates the shock induced separation zone. These are also in agreement with other computational and experimental data in literature.

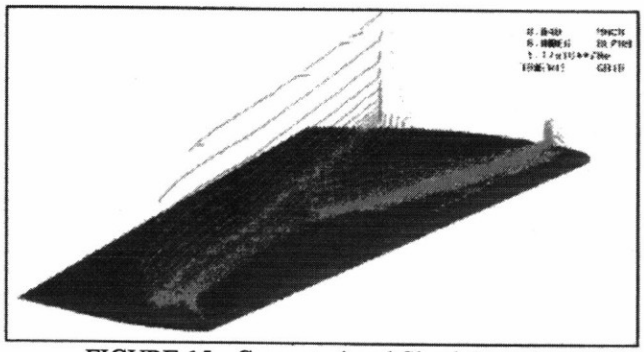

FIGURE 15 - Computational Shock Location on ONERA-M6 Wing for Case C

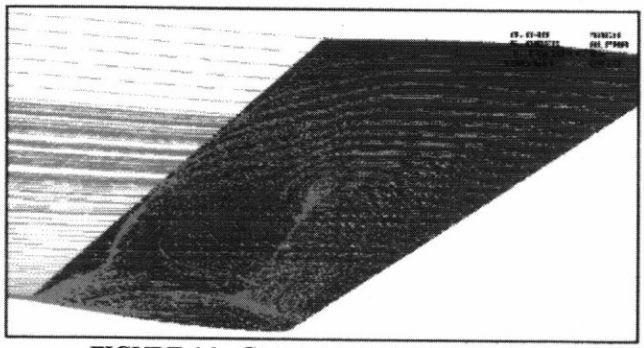

FIGURE 16 - Computational Particle Traces on ONERA-M6 Wing for Case C

Wing-Body Configuration

As another geometry, a wing-body configuration was selected. In order to compute the flow field around this geometry, the multi-block code was run both in inviscid and viscous mode. The comparisons were made with wind tunnel tests which contain selected data of surface pressure distributions. The experiments were done in RAE (Royal Aircraft Establishment in United Kingdom) 8 ft x 6 ft transonic wind tunnel on RAE research wing "A" in combination with an axisymmetric body [5]. Wing "A" is a wing of simple planform with no dihedral or twist and is based on a uncambered "RAE 101" airfoil. In the experiment, the test Reynolds number has been kept at 1×10^6 based on the geometric mean chord. The complete geometry definition of wing-body configuration is shown in Figure 17. In the experiment, the tunnel wall interference was relatively small. Although the tests have been made on a complete model of a size, the computations were performed by using only one-fourth of the configuration at zero angle of attack and one half of it at a non zero angle of attack. These were done due to mirror symmetry. The wake was modeled by extending the boattail up to X = 34.95 inch, turning the grid line parallel to the model axis and extending it to the downstream boundary. The computational grid was combined of five blocks as shown in Figure 18. For each block, the size of grid is presented in Table 5.

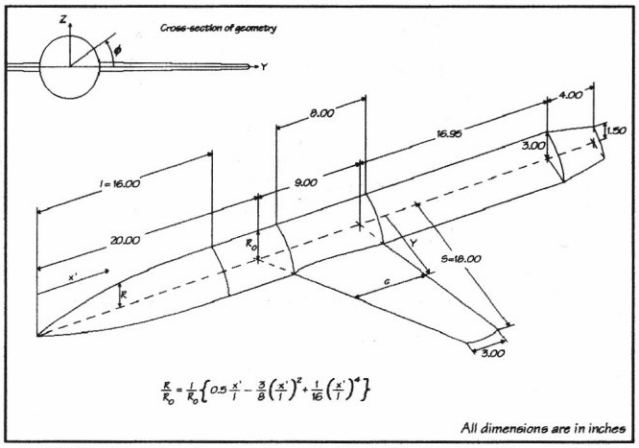

FIGURE 17 - Geometry of Wing-Body Configuration

The computations were done at Mach numbers 0.4 and 0.8 with angles of attack, $\alpha = 0.0^\circ$ and $\alpha = 2.0^\circ$. For zero angle of attack cases, the computational time for one converged solution is approximately sixty hours in DEC-Alpha 3000/800 workstation with 110 Mflops speed. If there is an angle of attack in the computation then the CPU time is doubled due to increase in the size of the grid. The comparison of computed and experimental surface pressure coefficients are presented from Figure 19 to 23.

Block #	ξ direction	η direction	ζ direction
1	25	21	65
2	17	21	65
3	41	21	65
4	25	21	65
5	41	21	65

TABLE 5 - Grid Dimensions in Each Zone

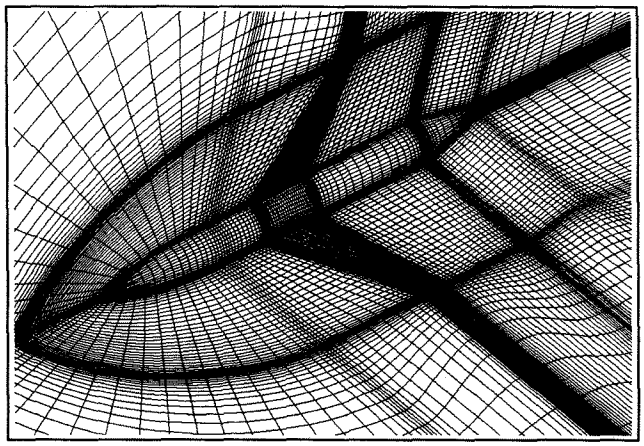

FIGURE 18 - Overall View of Computational Domain

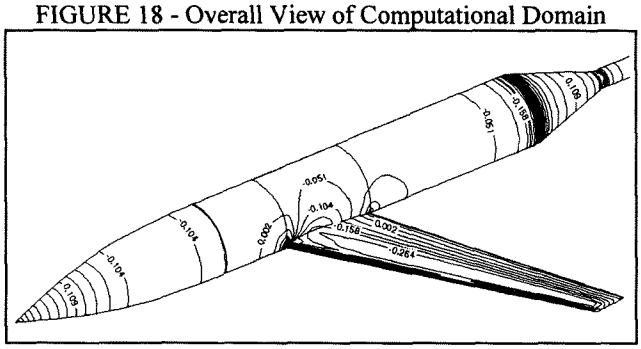

FIGURE 19 - Surface Pressure Coefficient Contours at $M_\infty = 0.4$, $\alpha = 0.0^\circ$

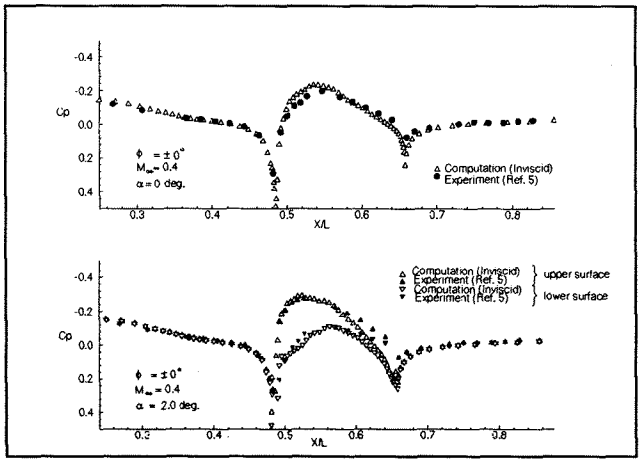

FIGURE 20 - Pressure Coefficient Distribution on Wing-Body Junction at $M_\infty = 0.4$

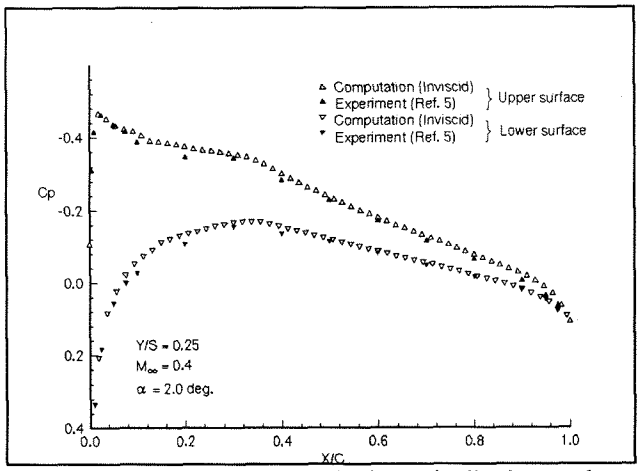

FIGURE 21a - Pressure Coefficient Distribution on the Wing at Spanwise Location Y/S=0.25 for $M_\infty = 0.4$

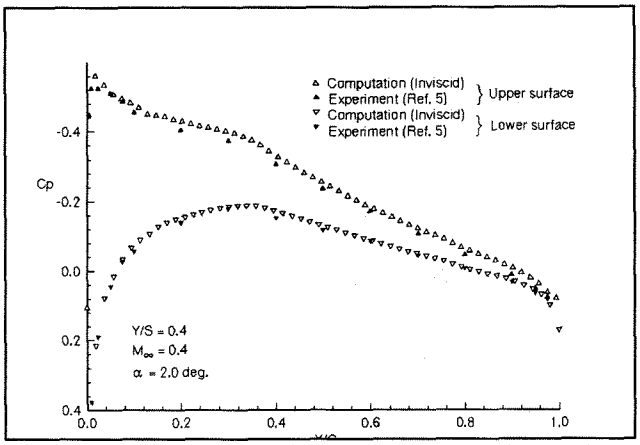

FIGURE 21b - Pressure Coefficient Distribution on the Wing at Spanwise Location Y/S=0.4 for $M_\infty = 0.4$

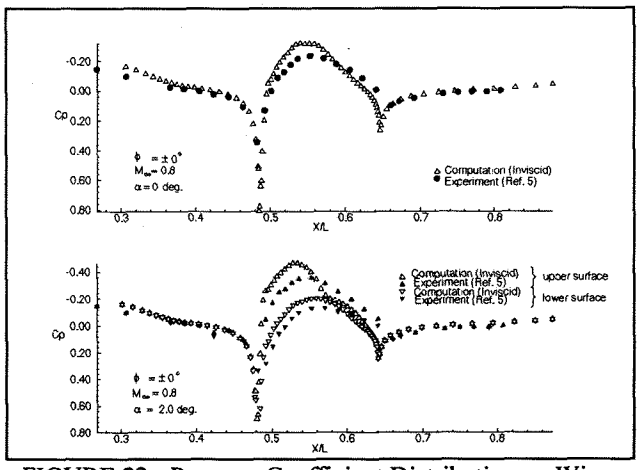

FIGURE 22 - Pressure Coefficient Distribution on Wing-Body Junction at $M_\infty = 0.8$

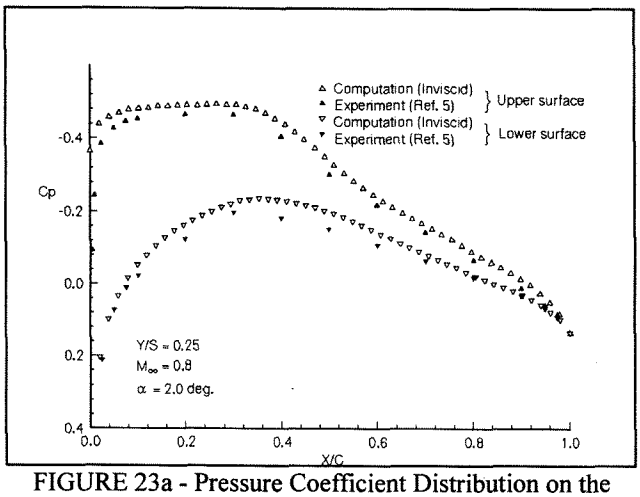

FIGURE 23a - Pressure Coefficient Distribution on the Wing at Spanwise Location Y/S=0.25 for $M_\infty = 0.8$

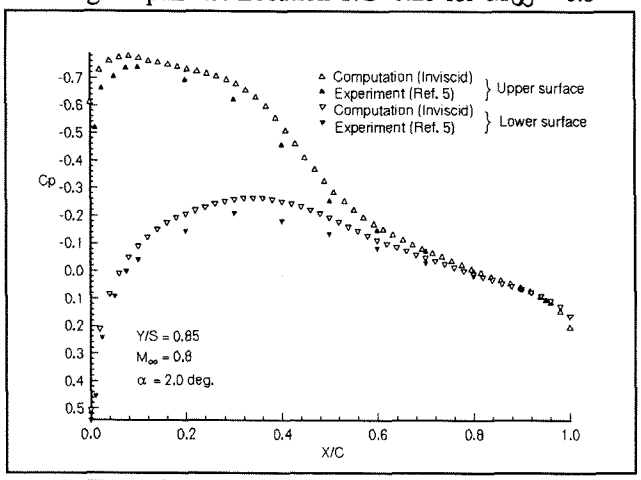

FIGURE 23b - Pressure Coefficient Distribution on the Wing at Spanwise Location Y/S=0.85 for $M_\infty = 0.8$

Wrap-Around Finned Missile

The last case was selected as a wrap-around finned missile. This type of configurations have been used widely due to their advantages in packaging and storage in tubular launchers. More missiles with wrap-around fins can be stored in the same volume than fixed finned missiles. Also wrap-around fins has great effects on the dynamic stability of the missile. The roll moment produced by fins may change in magnitude and sign more than once as the Mach number varies. This behavior can cause poor flight dynamics. In order to produce dynamically stable missile, the aerodynamic coefficients and also their derivatives for all stages of full flight have to be calculated correctly.

The flow field solutions of a wrap-around finned missile were obtained at zero angle of attack with various Mach numbers. The geometry definition of this configuration is given in Figure 24.

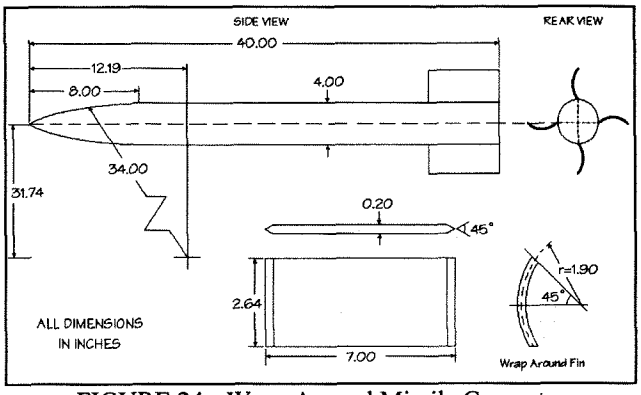

FIGURE 24 - Wrap-Around Missile Geometry

A sample computational grid around one fourth of the missile is shown in Figure 25. As the flow symmetry occurs at zero angle of attack, the computations were done by using a quarter of the full geometry. For this domain, the number of total grid size is 107×41×21. The Reynolds number varied from 4.6×10^6 to 9.0×10^6 based on the diameter in the Mach number range of 0.8 to 2.5. The elapsed time for a converged solution is approximately 24 hours in DEC-Alpha 3000/800 work station. The aerodynamic coefficients were compared with available experimental and computational results.The preliminary results for forebody axial force coefficient, C_X and rolling moment coefficient, C_l, given in Table 6 are in good agreement with the experimental data [14]. The Mach contours for two different free stream Mach numbers were given in Figures 26 and 27.

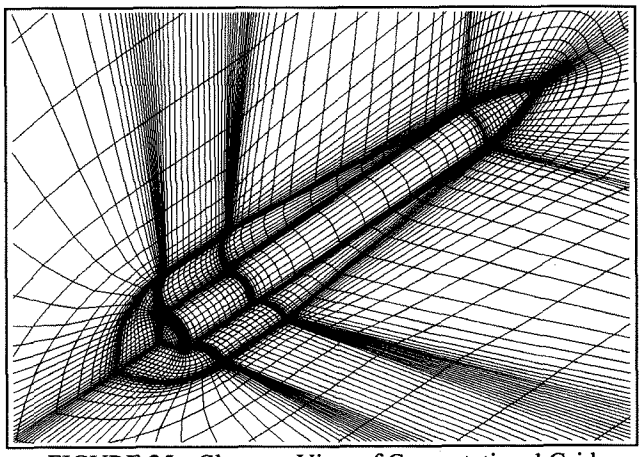

FIGURE 25 - Close up View of Computational Grid

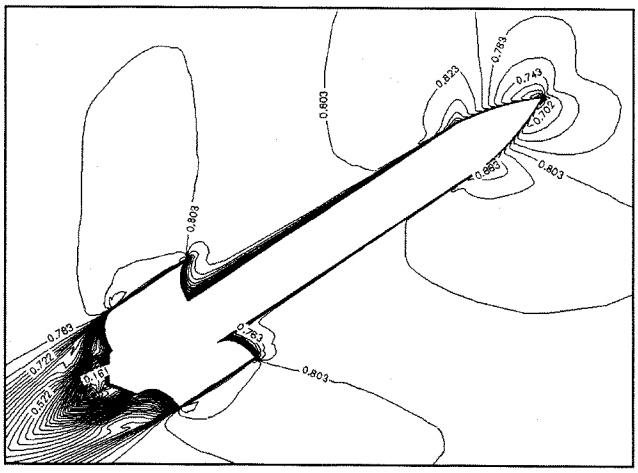

FIGURE 26 - Iso Mach Lines at M=0.80, α=0.0 deg.

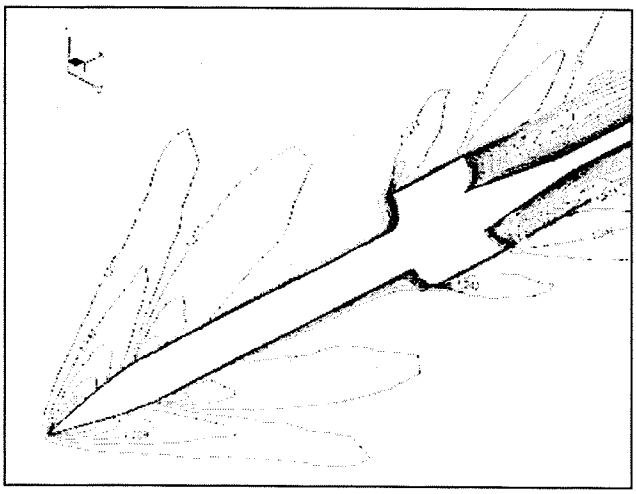
FIGURE 27 - Iso Mach Lines at M=1.30, α=0.0 deg

Aerodynamic Coefficients	Computation		Experiment	
	M=0.8	M=1.3	M=0.8	M=1.3
C_X	0.221	0.535	0.265	0.65
C_l	0.0128	-0.014	0.0122	-0.0065

TABLE 6 - Comparison of Aerodynamic Coefficients

Conclusion

From this study, one can conclude that the multi zone capability of the code is essential in solving flow problems involving complex and realistic geometries. Multi block approach also overcomes the difficulties encountered by the hardware limitations such as data storage and memory requirement.

Validating the code by comparing the numerical solutions with experimental data is necessary in order to make the CFD method a truly complementary engineering tool to wind tunnel testing. In this study the code validation was also done. For this purpose, various test cases were examined and were compared with different experimental and computational results from literature. The computations were found to agree well with the experimental and computational data.

The major disadvantage of the present method is that the grid generation must be done providing continuous block interfaces. This problem will be solved in order to get a more flexible design tool.

References

[1] Fujii, K., "Practical Applications of New LU-ADI Scheme for the Three Dimensional Navier-Stokes Computation of Transonic Viscous Flows," AIAA 24th Aerospace Sciences Meeting, Reno, Nevada, January, 1986.

[2] Beam, R. W., and Warming, R. F., "An Implicit Finite Difference Algorithm for Hypersonic Systems in Conservation Form," *Journal of Computaional Physics*, Vol. 23, 1976, pp 87-110.

[3] Steinbrenner, J. P., Karman, S. L., Jr., Chawner, J. R., "Generation of Multiple Block for Arbitrary Three Dimensional Geometries," General Dynamics, Fortworth Division, February, 1987.

[4] Baldwin, B. S., Lomax, H., "Thin Layer Approximation and Algebraic Model for Separated Turbulent Flows," AIAA 16th Aerospace Meeting, Huntsville, Alabama, January, 1978.

[5] Tradegold, D. A., Jones, A. F., Wilson, K. H., "Pressure Distribution in the RAE 8ftx6ft Transonic Wind Tunnel on RAE Wing 'A' in Combination with an Axisymmetric Body at Mach Numbers 0.4, 0.8 and 0.9," Royal Aircraft Establishment, Farnbrough, Hants, United Kingdom.

[6] Cebeci, T., Smith, A. M. O., " Analysis of Turbulent Boundary Layers, " Academic Press, 1974.

[7] Johnson, D. A., King, L. S., "A Mathematically Simple Turbulence Closure Model for Attached and

Separated Turbulent Boundary Layers, " AIAA Journal, Vol.23, No. 11, 1985.

[8] Harris, C. D., " Two Dimensional Aerodynamic Characteristics of the NACA0012 Airfoil in the Langley 8-ft. Transonic Pressure Tunnel, " NASA TM-81927, 1981.

[9] Van Den Berg, B., Gooden, J.H.M., "Low Speed Surface Pressure and Boundary Layer Measurement Data for the NLR7301 Airfoil Section with Trailing Edge Flap, " AR303, A9, 1994

[10] Stallings, R. L., Jr., Lamb, M., "Wing-Alone Aerodynamic Characteristics for High Angles of Attack at Supersonic Speeds," NASA TP-1889, 1981.

[11] Chan, J. S.," Viscous Supersonic Flow Computations over a Delta-Rectangular Wing with Slanting Surfaces," *Journal of Spacecraft and Rockets*, Vol.28, No.2, 1992, pp 615-620.

[12] Schmitt, V and Charpin, F., " Pressure Distributions on Onera-M6 Wing at Transonic Mach Numbers, " Office National D'Etudes Recherches Aerospatiales, 92320, Chatillon, France.

[13] Rumsey, C. L., Vatsa, V. N., " A Comparison of the Predictive Capabilities of the Several Turbulence Models Using Upwind and Central Difference Computer Codes, " AIAA 31st Aerospace Sciences Meeting and Exhibit, Reno, Nevada, January 11-14, 1993.

[14] Dahlke, C. W., et al., " Aerodynamic Characteristics of Wrap-Around Fins Mounted on Bodies of Revolution and Their Influence on the Missile Static Stability at Mach Numbers from 0.3 to 1.3," Vol.1-2, Army Missile Command, Redstone Arsenal, Alabama, April, 1972.